A model of mitochondrial ATP synthase deficiencies. The role of mitochondrial carriers.

Jean-Pierre Mazat [1,2,*], Anne Devin [1], Edgar Yoboue [2] and Stéphane Ransac [1,2]

[1] UMR 5095, IBGC CNRS, 1 Rue Camille Saint-Saens 33077, Bordeaux Cedex, France
[2] Université de Bordeaux, 146 Rue Leo-Saignat, 33076 Bordeaux Cedex, France
* Correspondence: jean-pierre.mazat@u-bordeaux.fr

Abstract: The m.8993T>G mutation of the mitochondrial *MT-ATP6* gene is associated with NARP syndrome (Neuropathy, Ataxia and Retinitis Pigmentosa). The equivalent point mutation introduced in yeast *Saccharomyces cerevisiae* mitochondrial DNA considerably reduced the activity of ATP synthase and of cytochrome-C-oxidase preventing yeast growth on oxidative substrates. The overexpression of the mitochondrial oxodicarboxylate carrier (Odc1p) is able to rescue the growth on oxidative substrate in stimulating the substrate-level phosphorylation of ADP coupled to conversion of α-ketoglutarate (AKG) into succinate with an increase in Complex IV activity. In order to better understand the mechanism of ATP synthase mutation bypass, we developed a core model of mitochondrial metabolism based on AKG as respiratory substrate. We describe the different possible metabolite output and the ATP/O ratio values as a function of ATP synthase inhibition.

Keywords: Mitochondrial metabolism; Metabolic Model; ATP/O; substrate level phosphorylation; Odc1;

---

1. Introduction

Mitochondria support aerobic respiration and produce most of cellular ATP by oxidative phosphorylation, i.e. the coupling of a series of redox reactions, the electron transport chain (ETC) with the ATP synthase through a transmembraneous proton gradient. The ETC is mainly fed by the NADH and succinate generated in the TCA cycle and some other possible dehydrogenases.

The ATP synthase organizes into a matrix domain (F1 inside mitochondria) where ATP is synthesized and a membrane-embedded domain (Fo) that moves protons across the membrane **[1,2]**. Dozens of point mutations in the mitochondrial MT-ATP6 gene (ATP6 in yeast) have been identified as leading to deleterious neuromuscular disorders **[3]**. The m.8993T>G mutation of the mitochondrial MT-ATP6 gene affecting mitochondrial energy transduction has been particularly studied **[4]**. This mutation has been associated in human with numerous cases of neuropathy, ataxia and retinitis pigmentosa (NARP) and maternally inherited Leigh syndrome.

The equivalent mutations introduced in the yeast *Saccharomyces cerevisiae* (NARP mutant) **[5]** dramatically slow down its respiratory growth. It was recently shown that this mutation prevents proton release in the mitochondrial matrix strongly decreasing ATP synthesis to 10% of the wild type (WT) value **[6]**. Concomitantly with the ATP synthase defect, a decrease in Complex IV amount is observed (retrograde signaling pathway linking ATP synthase and complex IV biogenesis **[4,7,8]**).

An additional molecule of ATP (in yeast) or GTP (in liver) is produced in TCA cycle by Succinyl-CoA synthetase, also named succinate thiokinase. It is called substrate level phosphorylation (SLP) as it occurs in glycolysis. Following the pioneer work of Schwimmer et al. **[7]**, a rescue of the NARP mutation in yeast was mediated through the mito chondrial carrier Odc1p overexpression **[4]**. Odc1p is a mitochondrial carrier able to exchange 2-oxoglutarate (AKG) against succinate, malate or citrate (and several other metabolites, not a priori involved in the rescuing process) **[9]**. The Odc1p overexpression presumably increases AKG uptake in mitochondria with succinate or malate exchange promoting the subsequent increase in ATP synthesis by SLP (SLP-ATP) **[7]**. In both cases the rescue is accompanied by an increase of complex IV amount without nevertheless reaching the WT value.

Odc1p carrier was identified and characterized by Palmieri et al. **[9]**. It operates by a strict counter exchange mechanism. Odc1p carrier can principally uptake 2-oxoglutarate against itself (112.5), succinate (19), malate (56) and citrate (28.6). The numbers in brackets indicate in mmol/min/g protein the rate of 2-oxoglutarate uptake in proteoliposomes preloaded with the corresponding metabolite (table II in **[9]**). The diversity of output catalyzed by Odc1p offers different metabolic solutions to enhance SLP-ATP. In order to have a better understanding of the rescue mechanism by Odc1p we develop in this paper a metabolic model of yeast mitochondria that allows to characterize the different possible metabolic pathways bypassing ATP deficiency in isolated yeast mitochondria using α-ketoglutarate (AKG) as respiratory substrate.

2. Materials and Methods

Two similar models, detailed in supplementary materials S1 and S2, were developed, one for the calculation of the EFM (Elementary Flux Modes, i.e. the minimal set of fluxes at steady state of the metabolic network), the other in which the incorporation of rate equations allows a more precise study of the dynamics of the metabolic fluxes.

Both models involve a relevant representation of the coupling between respiratory chain and ATP synthesis through a chemiosmotic proton gradient $\Delta\mu H^+$ considered here as a pseudo substrate called PMF (for Proton Motive Force). For those reactions which depend only on the ΔpH or on the $\Delta\psi$ component of the $\Delta\mu H^+$, we take, following Bohnensack [10], $\Delta pH = 0.2$ PMF and $\Delta\psi = 0.8$ PMF.

Both models include the different exchanges catalyzed by Odc1p under the form of 3 reactions for AKG input:

T2 : AKGc + MALm = AKGm + MALc .

T22 : AKGc + SUCCm = AKGm + SUCCc .

T23 : AKGc + CITm = AKGm + CITc .

In addition there is in yeast mitochondria the dicarboxylate carrier (DIC) which can catalyze the exchanges:

T31 : MALm + Pic = MALc + Pim .

T33 : SUCCm + Pic = SUCCc + Pim .

3. Results

The aim of the model is to simulate the experiments on isolated yeast mitochondria with 10 mM AKG as respiratory substrate and to characterize all possible metabolic pathways inside mitochondria, and metabolite outputs including ATP synthesis. We also study the oxygen consumption flux and calculate the ATP/O ratio for which experimental results already exist [11] .

In a first part we will describe the Elementary Flux Modes (EFMs) i.e. the minimal pathways at steady-state inside a metabolic network [12]. In this context, minimal means that the removal of a step prevents the establishment of a steady state. They either connect input with output metabolites or are cycles at steady-state. Any set of fluxes at steady-state in a metabolic network can be written as a linear combination of EFMs. Thus the EFMs present all the salient features of a metabolic network making them a powerful tool in metabolic studies.

3.1. Determination of EFMs with 2-Oxoglutarate (AKG) as respiratory substrates

The EFMs of Model 1 where determined using Metatool [13]. The direction of the carriers in Model 1 are such that only AKG is allowed as respiratory substrate. In these conditions, we obtain 59 EFMs. Among these 59 EFMs, 8 involve the entry of only AKG, ADP, Pi and O, and the output of ATP (represented in Fig. 1 and in supplementary Materials S3). The outputs are succinate only (EFMs 28 and 17, Fig. 1 a and d respectively), malate only (EFMs 29 and 20, Fig. 1b and e respectively), malate + citrate (EFMs 30 and 23, Fig.1c and f), Succinate + citrate (EFM 42, Fig. 1g) or succinate + malate (43, Fig. 1i). The EFMs 17, 20 and 23 involve a membrane leak (L) which consumes the PMF without ATP synthesis (ASYNT = 0) with a rather low ATP/O of 0.5 or 1. There is a last EFM without oxygen consumption, EFM 4 represented in Fig. 1h. This EFM involves the reversion of ATP synthase (-ASYNT). Even if an oxygen consumption is experimentally observed, this EFM cannot be excluded because it can participate to a linear combination of EFMs, with a net consumption of oxygen. All in all the ATP/O values range

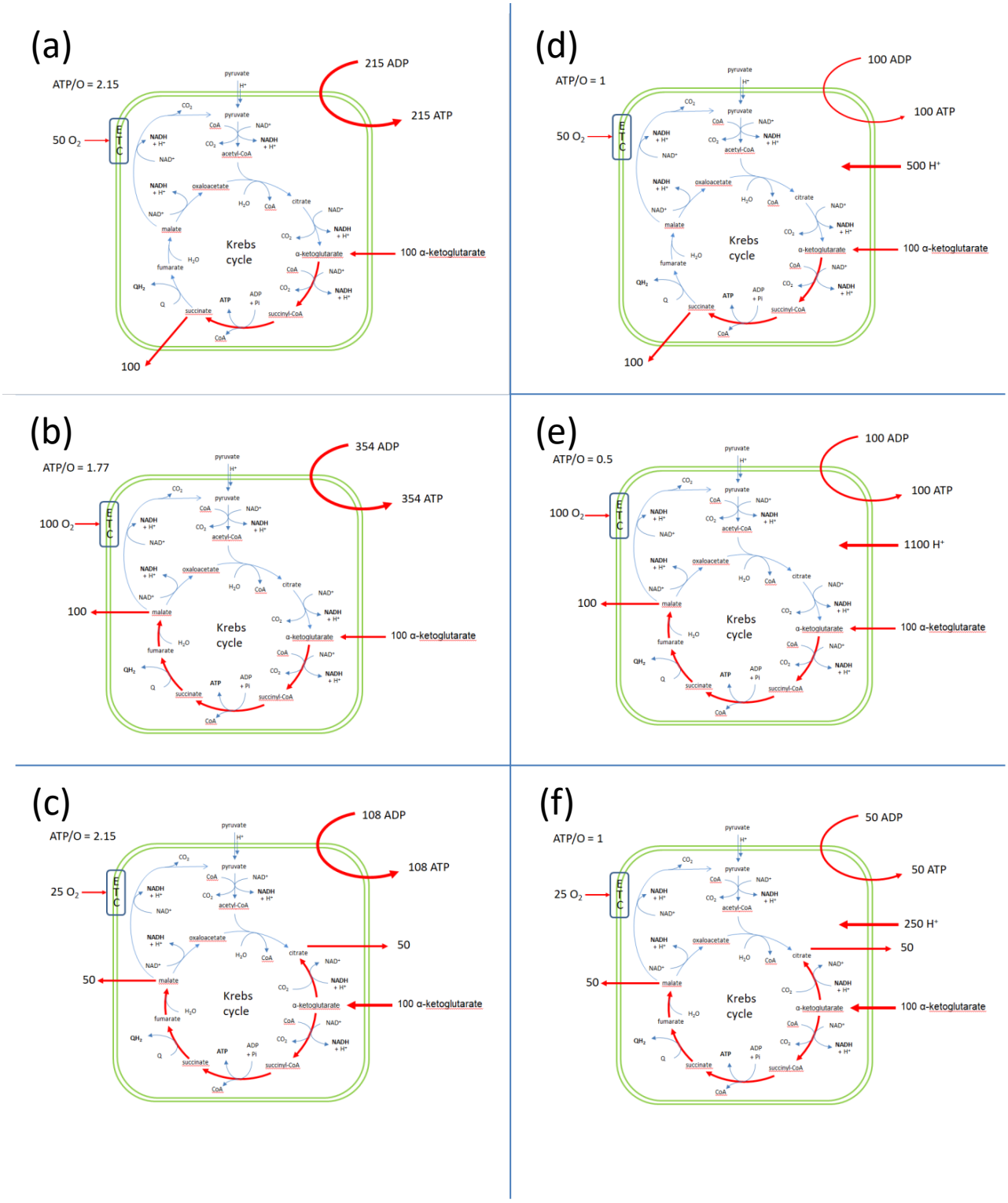
(a)
ATP/O = 2.15
215 ADP
215 ATP
50 O2
100 α-ketoglutarate
100
(d)
ATP/O = 1
100 ADP
100 ATP
50 O2
500 H+
100 α-ketoglutarate
100
(b)
ATP/O = 1.77
354 ADP
354 ATP
100 O2
100
100 α-ketoglutarate
(e)
ATP/O = 0.5
100 ADP
100 ATP
100 O2
1100 H+
100
100 α-ketoglutarate
(c)
ATP/O = 2.15
108 ADP
108 ATP
25 O2
50
50
100 α-ketoglutarate
(f)
ATP/O = 1
50 ADP
50 ATP
25 O2
250 H+
50
50
100 α-ketoglutarate
Krebs cycle
ETC

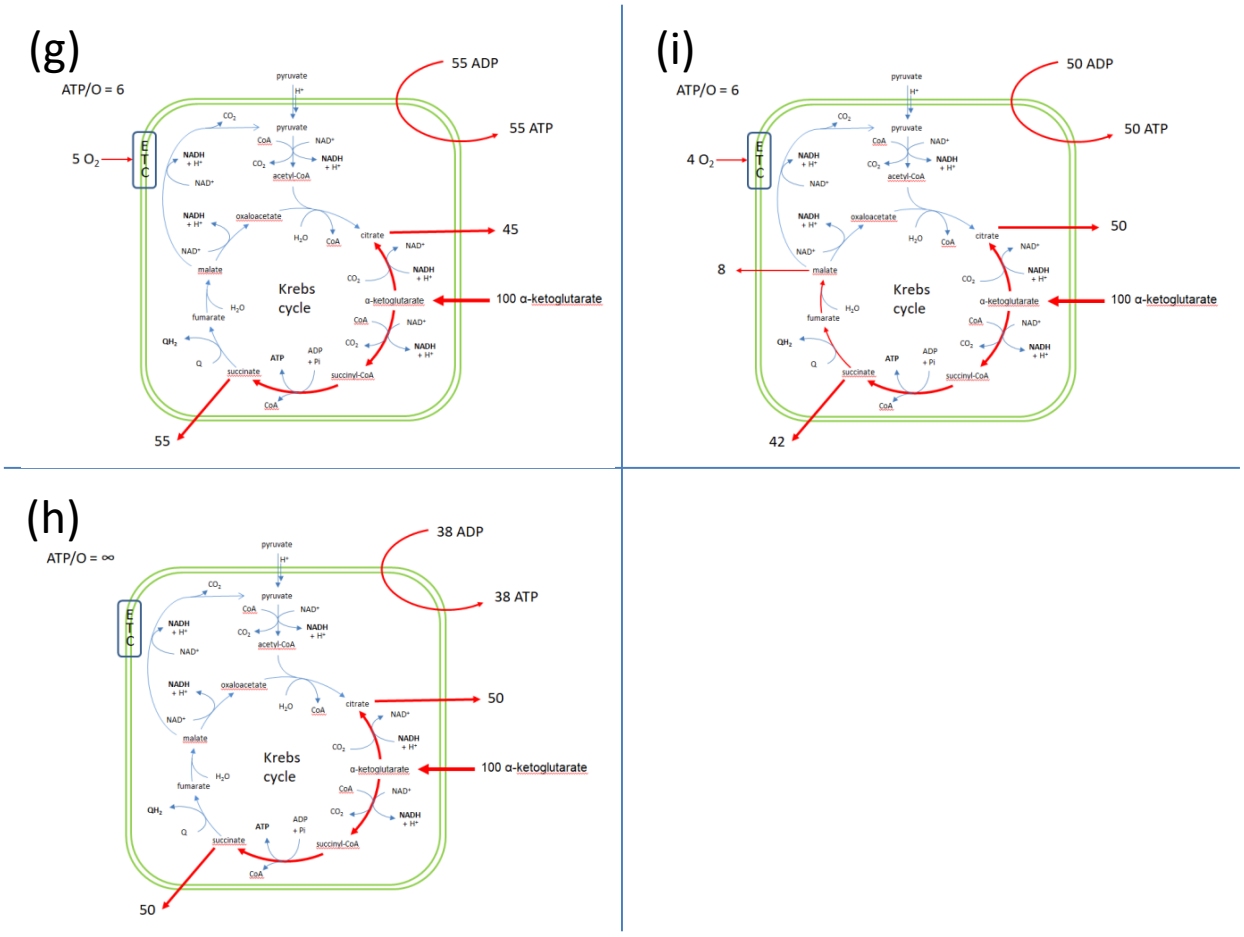

Figure 1. Schematic representation of the EFMs able to explain the set of fluxes in isolated yeast mitochondria respiring on AKG. (d), (e) and (f) correspond to a consumption of PMF through the leak L. All the values are given for an input of 100 AKG per time unit (in arbitrary units) in order to facilitate the comparison of the release fluxes. The EFMs are detailed in Supplementary Material S3.

from 0.5 to 6. Two EFMs (EFM 28 and EFM 30) display an ATP/O of 2.15 close to the published value of 2.3 [7,11]. However because the actual fluxes in a metabolic network can be seen as a linear combination of EFMs, the experimental value of 2.3 can result from a combination of different EFMs with different ATP/O values. Thus, any of the 9 EFMs can be implicated either alone (EFMs 28 and 30) or in combination.

In order to get more insight in the actual metabolic fluxes and the pathway taken by AKG inside the mitochondria, we develop a kinetic model using Copasi [14] involving the kinetic properties known for each step as described in supplementary material S2 with kinetic parameters listed in supplementary material S4.

Of note, Copasi can also calculate the EFMs but only with integer stoichiometric coefficients which necessitates to write the enzymatic reactions with high stoichiometric coefficients, particularly for ATP synthase which uses 10 protons to make 3 ATP and for those reactions which use $\Delta pH = 0.2$ PMF and $\Delta\psi = 0.8$ PMF. We got exactly the same results with Copasi as with Metatool.

3.2. Dynamics of oxygen consumption and ATP generation and determination of the ratio ATP/O as a function of ATPsynthase activity (Fig. 2).

Three properties of the model must be emphasized.

1) Because the thermodynamic span between the pair NADH/NAD and QH_2/Q is much broader than the span between succinate/fumarate and QH_2/Q, NADH is oxidized before QH_2 (Fig. 2b) so that the accumulation of QH_2 blocks the respiratory complex II (RCII or SDH).

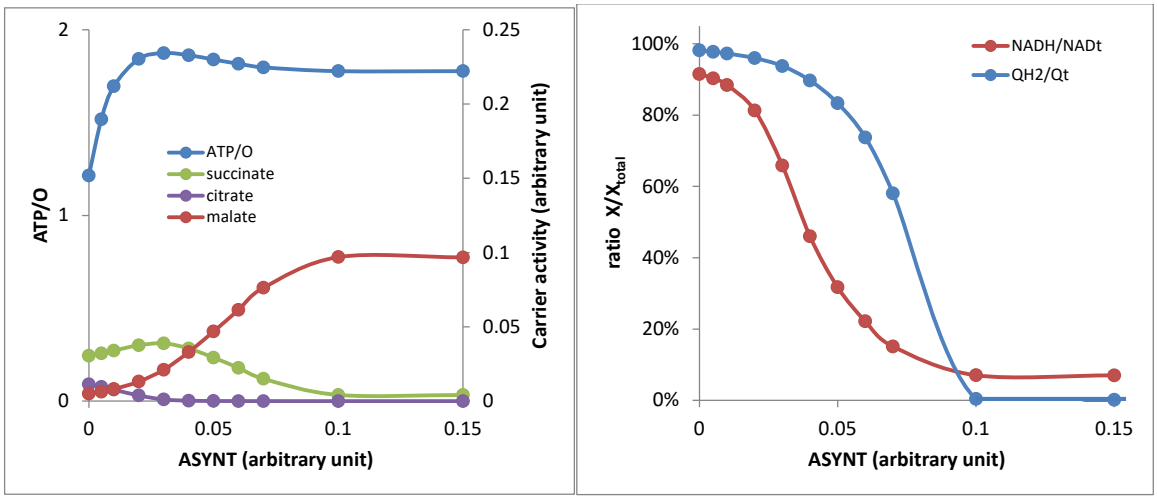

Figure 2. Energy metabolism of isolated yeast mitochondria respiring on AKG as a function of ATP synthase activity. (a) ATP/O ratio (left scale) and output fluxes in arbitrary units (right scale); (b) NADH/NAD and QH_2/Q ratios. The parameters of the kinetic model are listed in Supplementary Materials S4.

2) When the ratio NADH/NAD is high (low activity of ATP Synthase) the reversion of IDH3 associated with NADH reoxidation is possible.

3) When both NADH/NAD and QH_2/Q ratios are low (high activity of respiratory chain), RCII is active and succinate is easily transformed in fumarate competing with the output of succinate against AKG through Odc1p. The AKG/succinate exchange is thus decreased and replaced by the AKG/malate exchange (Fig. 2a at high ASYNT activity).

Let us now describe the behavior of the mitochondrial metabolism with AKG as respiratory substrate as a function of ATP synthase activity (corresponding to different degrees of activity or different amount of the ATP synthase inhibitor oligomycin) (Fig.2). When ASYNT = 0 the respiratory chain is slowed down by the PMF leading to high NADH/NAD and QH_2/Q ratios. The RCII activity is very low so that the succinate goes out against AKG. The high NADH level reverses the IDH3 activity leading to citrate output against AKG. There is a very low malate output in these conditions). An ATP/O = 1.2 is obtained which fit well with the 1.1 value experimentally observed [11].

At an intermediate ASYNT value of 0.04, the respiratory chain becomes active and consumes NADH (Figure 2b). The NADH decrease prevents IDH3 reversion and the production of citrate (Figure 2a). The slight decrease of QH_2 (10%) allows an increase in malate production, but succinate output remains high. An ATP/O = 1.9 is observed in these conditions.

At higher ASYNT activity above 0.1 (WT), NADH and QH_2 concentrations become low liberating the RCII activity which consumes nearly all synthesized succinate. There is no longer an output of succinate which is metabolized in malate excreted against AKG. The ATP/O is equal to 1.8, a bit lower than the observed value of 2.3. We will discuss this point later.

Table 1. ATP synthesis, respiration and ATP/O in wild type (WT), NARP mutation and NARP + 10 times Odc1p overexpression calculates with Copasi model in arbitrary units.

No Odc1p leak	ATP synthesis rate	Respiration rate	ATP/O
WT	0.297	0.167	1.77
NARP	0.033	0.027	1.22
NARP + Odc1p (x10)	0.074	0.033	2.22

4. Discussion

In this paper, we introduced a metabolic model of yeast mitochondria respiring on AKG to try to understand the basis of the rescue of ATP synthase mutants by Odc1p and the constraints in this metabolic bypass.

The description of the EFMs, i.e. the minimal pathways in the metabolic network, shows that, in principle, any TCA segment can be taken from AKG leading to any TCA intermediate output (Fig. 1) with ATP/O ratios ranging from 0.5 to 6 except for EFM of Fig. 1h, for which there is no oxygen consumption. The already reported ATP/O ratio of 2.4 [11] is close to the one of 2.15 measured in EFMs of Fig.1a and c which correspond in our system to an exit of succinate on the one hand or malate and citrate on the other hand. However the metabolic fluxes at steady state of the isolated mitochondria respiring on AKG can be the combination of several EFMs with different ATP/O leading to the 2.4 value. This shows that different combination of EFMs i.e. different combinations of ASYNT-ATP and SLP-ATP can lead to the ATP/O values measured experimentally.

To get insight in this matter, we introduced in our model the rate equations of the different steps and we studied the steady state of the metabolic network at different ATP synthase activity values. We observed a rewiring of mitochondrial metabolism when the amount of ATP synthase is decreased with an ATP/O passing from a value of 1.8-1.9 to a value of 1.2 close to the corresponding experimental values 1.1 reported in [11] in presence of oligomycin, an inhibitor of ATP synthase. However, one may wonder the reason(s) of the difference between the theoretical value of 1.8 and the experimental one of 2.4 at high ATP synthase activity. As we noticed earlier, two EFMs present an ATP/O of 2.15 close to the experimental value. One presents an output of citrate which is not observed in our kinetic model at high ATP synthase activity. The other one supposes that all AKG entry occurs in exchange with succinate output. As discussed above, succinate output necessitates that SDH (complex II) is inactive which in our case is obtained at high QH_2 concentration. Another solution can come from the participation of EFMs with ATP/O = 6. Once more these EFMs involve a citrate output which necessitates high NADH concentration. This is not the case at high ATP synthase concentration in our kinetic model in which the release of metabolites changed from malate at high ATP synthase activity to succinate and ultimately, at null ATP synthase activity, to mainly succinate release, and marginally citrate and malate release. Experimental characterization of the metabolites outputs is under way to solve this discrepancy.

Curiously, in our model the effect of increasing the activity of Odc1p carrier (x 10) is rather weak (table 1, No Odc1 leak). This could be explained by several factors. First, the growth of NARP + Odc1p is much less than the growth of the wild type (Figure 1 in [4]) suggesting that the increase in ATP synthesis with Odc1p overexpression is far from reaching the WT value ; second, it was shown that in the NARP mutant, the activity of complex IV the last step of respiratory chain is decreased by 80%, so that the 0.033 value of ATP synthesis in NARP (Table 1) is probably overestimated. The effect of Odc1p overexpression is not only to increase the expression of the carrier but also to increase the level of the complex IV (40% of the WT activity, table 1 in [4]) (retrograde signaling pathway linking ATP synthase and complex IV biogenesis [4,7,8]).

Another factor could play an important role in the rescue of NARP mutant by Odc1p overexpression. One of the strong constraints of SLP-ATP production is the mandatory reoxidation of the NADH produced by α-ketoglutarate dehydrogenase, the reaction preceding the thiokinase reaction that produces ATP in TCA cycle. Several ways exist in mitochondria to reoxidize NADH [15]. One occurring at low activity of ATP synthase is the reversion of isocitrate dehydrogenase in the presence of high concentration of NADH leading to citrate output as shown in Fig. 2. The other classical one is the activation of the respiratory chain by consumption of the PMF by the ATP synthase. Another way to consume the PMF and NADH activating the TCA cycle and SLP is an increase in the membrane leak. In yeast this leak is naturally high leading to high state 4 and a mild coupling between respiration and ATP synthesis (table 1 in [4]).

As a matter of fact it has been shown that CCCP, an uncoupler of respiratory chain from ATP synthase activity can also rescue ATP deficiency [4].

Table 2. ATP synthesis, respiration and ATP/O in wild type (WT), NARP mutation and NARP + 10 times Odc1p overexpression with a leak attached to Odc1p. The calculation are performed using the Copasi model in arbitrary units.

Odc1 leak	ATP synthesis rate	Respiration rate	ATP/O
WT	0.296	0.168	1.77
NARP	0.039	0.038	1.02
NARP + Odc1p (x10)	0.091	0.055	1.67

We can hypothesize that part of the Odc1p effect could be to increase the membrane leak favoring SLP-ATP not only by increasing AKG feeding part of the TCA cycle producing ATP but also NADH consumption by an activated respiratory chain. We tested this hypothesis in our model that showed that increasing the leak in the NARP + Odc1p conditions increased ATP synthesis (table 2).
Several reports show that substrate level phosphorylation is able to rescue ATP synthase deficiency or to favor ATP production in cell fed with glutamine, a precursor of AKG [16–18]. Our theoretical study evidences the constraints in enhancing SLP through a rewiring of energy metabolism. It also evidences the (perhaps multifactorial) role of the mitochondrial carriers such as Odc1p. The measurement of the metabolites releases should help understanding the metabolic pathways taken in ATP synthase rescue to find other possible way to bypass this deficiency.

Supplementary Materials: The following are available online at www.mdpi.com/xxx/s1, Model S1; Model S2; S3, list of EFMs of Fig.1; S4, list of the kinetic parameters used in Copasi model.

Funding: This work was supported by AFM, contract N° 218302 MitoBAD and EMERGENCE GSO.

Acknowledgments: This work beneficiated from helpful discussions with Stéphane Duvezin-Caubet, Jean-Paul di Rago, Michel Rigoulet and Déborah Tribouillard-Tanvier

Conflicts of Interest: The authors declare no conflict of interest.

Abbreviations

AKG: α-ketoglutarate / 2-oxoglutarate.
ASYNT-ATP: ATP synthesized by the mitochondrial ATP-synthase.
PMF: Proton Motive Force ($\Delta\mu H^+$).
SLP: substrate level phosphorylation.
SLP-ATP: ATP synthesized by Succinyl-CoA synthetase (suucinate thiokinase).

References

1. Zhou, A.; Rohou, A.; Schep, D.G.; Bason, J.V.; Montgomery, M.G.; Walker, J.E.; Grigorieff, N.; Rubinstein, J.L. Structure and Conformational States of the Bovine Mitochondrial ATP Synthase by Cryo-EM. *Elife* **2015**, *4*, e10180, doi:10.7554/eLife.10180.

2. Dautant, A.; Velours, J.; Giraud, M.-F. Crystal Structure of the Mg·ADP-Inhibited State of the Yeast F1c10-ATP Synthase. *J Biol Chem* **2010**, *285*, 29502–29510, doi:10.1074/jbc.M110.124529.

3. Dautant, A.; Meier, T.; Hahn, A.; Tribouillard-Tanvier, D.; di Rago, J.-P.; Kucharczyk, R. ATP Synthase Diseases of Mitochondrial Genetic Origin. *Front Physiol* **2018**, *9*, 329, doi:10.3389/fphys.2018.00329.

4. Su, X.; Rak, M.; Tetaud, E.; Godard, F.; Sardin, E.; Bouhier, M.; Gombeau, K.; Caetano-Anollés, D.; Salin, B.; Chen, H.; et al. Deregulating Mitochondrial Metabolite and Ion Transport Has Beneficial Effects in Yeast and Human Cellular Models for NARP Syndrome. *Hum Mol Genet* **2019**, *28*, 3792–3804, doi:10.1093/hmg/ddz160.

5. Rak, M.; Tetaud, E.; Duvezin-Caubet, S.; Ezkurdia, N.; Bietenhader, M.; Rytka, J.; di Rago, J.-P. A Yeast Model of the Neurogenic Ataxia Retinitis Pigmentosa (NARP) T8993G Mutation in the Mitochondrial ATP Synthase-6 Gene. *J Biol Chem* **2007**, *282*, 34039–34047, doi:10.1074/jbc.M703053200.

6. Su, X.; Dautant, A.; Rak, M.; Godard, F.; Ezkurdia, N.; Bouhier, M.; Bietenhader, M.; Mueller, D.M.; Kucharczyk, R.; di Rago, J.-P.; et al. The Pathogenic m.8993 T > G Mutation in Mitochondrial ATP6 Gene Prevents Proton Release from the Subunit c-Ring Rotor of ATP Synthase. *Hum Mol Genet* **2021**, *30*, 381–392, doi:10.1093/hmg/ddab043.

7. Schwimmer, C.; Lefebvre-Legendre, L.; Rak, M.; Devin, A.; Slonimski, P.P.; di Rago, J.-P.; Rigoulet, M. Increasing Mitochondrial Substrate-Level Phosphorylation Can Rescue Respiratory Growth of an ATP Synthase-Deficient Yeast. *J Biol Chem* **2005**, *280*, 30751–30759, doi:10.1074/jbc.M501831200.

8. Butow, R.A.; Avadhani, N.G. Mitochondrial Signaling: The Retrograde Response. *Molecular Cell* **2004**, *14*, 1–15, doi:10.1016/S1097-2765(04)00179-0.

9. Palmieri, L.; Agrimi, G.; Runswick, M.J.; Fearnley, I.M.; Palmieri, F.; Walker, J.E. Identification in Saccharomyces Cerevisiae of Two Isoforms of a Novel Mitochondrial Transporter for 2-Oxoadipate and 2-Oxoglutarate. *J Biol Chem* **2001**, *276*, 1916–1922, doi:10.1074/jbc.M004332200.

10. Bohnensack, R. Control of Energy Transformation of Mitochondria. Analysis by a Quantitative Model. *Biochim Biophys Acta* **1981**, *634*, 203–218, doi:10.1016/0005-2728(81)90139-0.

11. Rigoulet, M.; Velours, J.; Guerin, B. Substrate-Level Phosphorylation in Isolated Yeast Mitochondria. *Eur J Biochem* **1985**, *153*, 601–607, doi:10.1111/j.1432-1033.1985.tb09343.x.

12. Schuster S; Hilgetag, C. On Elementary Flux Modes in Biochemical Reaction Systems at Steady State. *J. Biol. Syst.* 1994, 165–182.

13. Pfeiffer, T.; Sánchez-Valdenebro, I.; Nuño, J.C.; Montero, F.; Schuster, S. METATOOL: For Studying Metabolic Networks. *Bioinformatics* **1999**, *15*, 251–257, doi:10.1093/bioinformatics/15.3.251.

14. Hoops, S.; Sahle, S.; Gauges, R.; Lee, C.; Pahle, J.; Simus, N.; Singhal, M.; Xu, L.; Mendes, P.; Kummer, U. COPASI--a COmplex PAthway SImulator. *Bioinformatics* **2006**, *22*, 3067–3074, doi:10.1093/bioinformatics/btl485.

15. Chinopoulos, C. Acute Sources of Mitochondrial NAD+ during Respiratory Chain Dysfunction. *Experimental Neurology* **2020**, *327*, 113218, doi:10.1016/j.expneurol.2020.113218.

16. Chinopoulos, C.; Seyfried, T.N. Mitochondrial Substrate-Level Phosphorylation as Energy Source for Glioblastoma: Review and Hypothesis. *ASN Neuro* **2018**, *10*, 1759091418818261, doi:10.1177/1759091418818261.

17. Sgarbi, G.; Casalena, G.A.; Baracca, A.; Lenaz, G.; DiMauro, S.; Solaini, G. Human NARP Mitochondrial Mutation Metabolism Corrected with Alpha-Ketoglutarate/Aspartate: A Potential New Therapy. *Arch Neurol* **2009**, *66*, 951–957, doi:10.1001/archneurol.2009.134.

18. Chen, Q.; Kirk, K.; Shurubor, Y.I.; Zhao, D.; Arreguin, A.J.; Shahi, I.; Valsecchi, F.; Primiano, G.; Calder, E.L.; Carelli, V.; et al. Rewiring of Glutamine Metabolism Is a Bioenergetic Adaptation of Human Cells with Mitochondrial DNA Mutations. *Cell Metab* **2018**, *27*, 1007-1025.e5, doi:10.1016/j.cmet.2018.03.002.

Supplementary Material S1: MITOY_AKG_12_in.dat => MITOY_AKG_12_out

```
-ENZREV
ANT ASYNT FUMARASE IDH3 MDH2 ME2 NIG RC3 SUCTHIOK T5 T6 T12 T24 T41 T42

-ENZIRREV
AKGDH ATPASE CS L NDI PDH RC2 RC4 T2 T22 T23 T31 T33

-METINT
ACoAm ADPc ADPm AKGc AKGm ATPc ATPm CITm CoAm Cyt_ox Cyt_red DPH DPSI FUMm MALm
NADm NADHm OAAm Pic Pim PYRm Q QH2 SUCCm SUCCoAm

-METEXT
ADP AKG ATP CITc CO2 H2O O MALc Pi PYRc SUCCc

-CAT
AKGDH : AKGm + NADm + CoAm = SUCCoAm + NADHm + CO2 .
ANT : ATPm + ADPc + DPSI = ATPc + ADPm .
ASYNT : 3 ADPm + 3 Pim + 10 DPH + 10 DPSI = 3 ATPm .
ATPASE : ATPc = ADPc + Pic .
CS : ACoAm + OAAm = CITm .
FUMARASE : FUMm = MALm .
IDH3 : CITm + NADm = AKGm + NADHm + CO2 .
L : DPSI + DPH = .
MDH2 : MALm + NADm = OAAm + NADHm .
ME2 : MALm + NADm = PYRm + NADHm + CO2 .
NIG : DPSI = 4 DPH .
PDH : PYRm + NADm + CoAm = ACoAm + NADHm + CO2 .
NDI : NADHm + Q = NADm + QH2 .
RC2 : SUCCm + Q = FUMm + QH2 .
RC3 : QH2 + 2 Cyt_ox = Q + 2 Cyt_red + 2 DPH + 2 DPSI .
RC4 : 2 Cyt_red + O = 2 Cyt_ox + 4 DPH + 4 DPSI + H2O .
SUCTHIOK : SUCCoAm + Pim + ADPm = SUCCm + CoAm + ATPm .
T2 : AKGc + MALm = AKGm + MALc .
T22 : AKGc + SUCCm = AKGm + SUCCc .
T23 : AKGc + CITm = AKGm + CITc .
T31 : MALm + Pic = MALc + Pim .
T33 : SUCCm + Pic = SUCCc + Pim .
T5 : Pic + DPH = Pim .
T6 : PYRc + DPH = PYRm .
T12 : Pic = Pi .
T24 : AKGc = AKG .
T41 : ADPc = ADP .
T42 : ATPc = ATP .
```

Supplementary Material S2:

INTRODUCTION.

According to [1], we define as global quantities in Copasi, 'fmu' which determines the part of Δψ (DpSI) in $\Delta\mu H^+$ (PMF). Here we take for simplicity: fmu = 0.8 and thus DPSI = fmu*PMF (Volts) and DPH = (1-fmu)*PMF/Z (in pH units).
We also define Z = ln(10)*RT/F ≈ 0.06 Volts at 30°C.

α-KETOGLUTARATE DEHYDROGENASE (AKGDH):

AKGm + NADm + CoAm -> SucCoAm + NADHm + CO2

It is supposed irreversible (ΔG°= -27.2 ± 7.7 kJ/mol => K'eq = 5.9×10^4) and inhibited by its products NADH and SucCoA. We propose an irreversible mass action law for the substrates, modulated by competitive inhibition terms for NADHm and SucCoAm with KAKGdh_NADH = 0.03 mM and KAKGdh_SucCoA = 10 µM taken from the literature [2–4]:

$$VM_{AKGDH}.AKGm.NADm.CoAm.\frac{1}{1+\frac{NADHm}{KAKGdh_NADH}}.\frac{1}{1+\frac{SucCoAm}{KAKGdh_SucCoA}}$$

or linearly written:
VM_AKGDH*AKGm*NADm*CoAm*(1/(1+NADHm/KAKGdh_NADH))*(1/(1+SucCoAm/KAKGdh_SucCoA))

ANT

We take the reversible mass action law with the intervention of DPSI = fmu*DPH

vANT = VM_ANT*(ADPc*ATPm-ADPm*ATPc*10^(-fmu*PMF/Z))

ASYNT

ATP SYNTHASE (ASYNT) :
ADPm + Pim + 3.3 * PMF = ATPm (stoichiometry of yeast Atp synthase: 10 H^+ per 3 ATP).
We took the expression of Bohnensack [1]:

$$VM_{ASYNT}.\left(1-\frac{ATPm}{ADPm.Pim}.Phi_p.10^{nA.\frac{PMFa-PMF}{Z}}\right)$$

where nA is the number of protons translocated per ATP synthesised (3.3 in the case of yeast), Phi_p takes into account the DPH in the phosphate ions equilibrium (see[1]) and PMFa is the standard phosphorylation potential (0.150 V) [1].

ATPASE : ATPc -> ADPc + Pic

We take a Henri-Michaelis-Menten equation [5] with the ATPc as substrate:

$$VM_ATPASE.\frac{\frac{ATPc}{KATPASE_ATP}}{1+\frac{ATPc}{KATPASE_{ATP}}}$$

CITRATE SYNTHASE (CS).

Acetyl-CoA (AcCoA) + Oxalacetate (0AA) + H_20 ⇌ Citrate + CoASH(CoA) + H^+ + 38 kJ/mol.

We consider the reaction as reversible and take the rate expression of Cornish-Bowden and Hofmeyr [6] with or without the inhibition by ATP (the inhibition by CoA is supposed to be included in the reverse rate)

$$V = \frac{\frac{VMCS.[OAAm]\times[ACoAm]}{KCS_OAA\times KCS_ACOA}\left(1-\frac{[CoA]\times[CITm]}{Kq_CS\times[ACoAm]\times[OAAm]}\right)}{\left[1+\frac{[OAA]}{KCS_OAA}+\frac{[AcCoA]}{KCS_ACOA}\left[1+\frac{ATP}{KiCS_ATP}\right].\right]\left[1+\frac{[CITm]}{KCS_CIT}+\frac{[CoA]}{KCS_COA}.\right]}$$

with the consensus values (in mM) : KCS_OAA = 0.005 ; KCS_ACOA = 0.01 ; KQ_CS = 2.10^6 (Veech JBC 1973) ; KiCS_ATP = 0.3 ; KCS_CIT = 3 ; KCS_COA = 0.04.

FUMARASE: FUMm = MALm

Reversible Henri-Michaelis-Menten equation which takes into account the equilibrium constant KQ_FUMASE = 4.4 in order to satisfy Haldane relationship:

(KFUMASE_FUM = 0.004 mM et KFUMASE_MAL = 0.009 mM)

$$VM_FUM.\frac{\left(\frac{FUMm}{KFUMASE_FUM}-\frac{MALm}{KQ_FUMASE.KFUMASE_FUM}\right)}{1+\frac{FUMm}{KFUMASE_FUM}+\frac{MALm}{KFUMASE_MAL}}$$

IDH3: ACONITASE-ISOCITRATE DEHYDROGENASE 3

Aconitase and isocitrate dehydrogenase are joined together in the reaction:

CITm + NADm = AKGm + NADHm + CO2

and the rate equation:

$$V = VM_IDH3\frac{\frac{.[CITm]\times[NADm]}{KI3_CIT\times KI3_NAD}\left(1-\frac{[AKGm]\times[NADHm]}{Kq_IDH3\times[CITm]\times[NADm]}\right)}{\left[1+\frac{[CITm]}{KI3_CIT}+\frac{[AKGm]}{KI3_NAD}\right]\times\left[1+\frac{[NADm]}{KI3_NAD}+\frac{[NADHm]}{KI3_NADH}.\right]}$$

LEAK: PMF -> PMFm

We take the equation:

$$\frac{VM_Leak}{1+\frac{KLEAK}{10^{\frac{PMF}{Z}}}}$$

Note that PMFm is created to satisfy the Copasi rules of writing the equations of the reactions. It is not a variable of the system.

MDH MALATE DEHYDROGENASE (Mitochondrial: MDH2):

MALm + NADm = OAAm + NADHm

Mass Action reversible with Keq = 0.0002

MALIC ENZYME (ME2):

Malate + NAD(P)+ ⇌ pyruvate + CO2 + NAD(P)H.

Mass action reversible with Keq (NAD ou NADPH) = 7.6 10^{-3}

NDI: NADHm + Q = NADm + QH2

In yeast, NDI is the internal dehydrogenase which takes the place of complex I in mammal's mitochondria. Because it does not excrete protons, its equilibrium constants K_{eq}= 4.10^{13} can be calculated from the difference in the Q/QH2 and NAD/NADH midpoint potentials (+0.085 V and -0.32 V respectively).

To satisfy this equilibrium constant we take k1 = 10 s^{-1} and k2 = 2.5 10^{-13} s^{-1} in a reversible mass action law.

PYRUVATE DEHYDROGENASE (PDH).
NAD^+ + CoA + Pyruvate ⇌ NADH + CO2 + Acetyl-CoA
We take the equation given in [7]. This reaction with a complex mechanism is taken as irreversible despite its ΔG° = -35.3 ± 6.4 kJ/mol (K'_{eq} = 1.6 × 10^6). We take into account an inhibition by the products NADH and acetyl-CoA (ACoA) (which is more or less equivalent to a reversible mechanism):

$$\frac{v}{V_{\max}} = \frac{PYRm}{KPDHPYR + PYRm} \times \frac{NADm}{KPDHNAD.(1+\frac{NADHm}{KiNADH}) + NADm} \times \frac{COAm}{KPDHCOA.(1+\frac{ACOAm}{KiACOA}) + COAm}$$

Pi TRANSPORT (Pit): Pic + H^+ = Pim
The electroneutral transport of Pi with a H^+ (or against OH^-) is very fast so that the phosphate distribution is supposed to be in equilibrium (taking into account the ΔpH).

According to[1] we take:

$$V_Pit = VM_Pit.\left(1 - \frac{Pim}{Pic}.10^{-DPH}\right) = VM_Pit.\left(1 - \frac{Pim}{Pic}.10^{-\frac{0.2.PMF}{Z}}\right)$$

or linearly written:

V_Pit = VM_Pit*(1-Pim/Pic*10^(-0.2*PMF/Z))

RCII (Respiratory complex II) or SDH (Succinate dehydrogenase):

In our simple dynamical model, we take the reversible mass action law as rate equation of the SDH with Keq = 70 calculated from the difference in the midpoint potentials of the pairs Fumarate/Succinate (E1 = +0.03 V) and Q/QH2 (E2 = + 0.085 V).

We adopt the rate equation of Cornish-Bowden and Hofmeyr [6] with a competitive inhibition of oxaloacetate with succinate and fumarate:

$$V = VM_SDH \times \frac{\dfrac{[SUCCm]\times[Q]}{KSDH_SUCC\times\left[1+\dfrac{[OAAm]}{KiSDH_OAA}\right]\times KSDH_Q}\left(1-\dfrac{[QH2][FUMm]}{KQ_SDH\times[SUCCm]\times[Q]}\right)}{\left[1+\dfrac{[SUCCm]}{KSDH_SUCC\times\left[1+\dfrac{[OAAm]}{KiSDH_OAA}\right]}+\dfrac{[FUMm]}{KSDH_FUM\times\left[1+\dfrac{[OAAm]}{KiSDH_OAA}\right]}\right]\times\left[1+\dfrac{[Q]}{KSDH_Q}+\dfrac{[QH2]}{KSDH_QH2}.\right]}$$

With the consensus values (for mammalian): KSDH_SUCC = 85 µM, K_{SDH_FUM} = 100 µM, K_{SDH_Q} = 1.5 µM (Grivennikova et al., [8]) and K_{SDH_QH2} = 1.5 µM (arbitrarily equal to K_M^Q = 1.5 µM in absence of known determination). KiSDH_OAA_ = 0.07 µM (0.01< <0.4); KQ_SDH = 0.14 (0.05< <0.5).

Note that oxaloacetate (OAAm) is not a metabolite of our model

RCIII or bc1 complex:

QH2 + 2 * Cox = Q + 2 * Cred + 2.4 * PMF
(4 protons (4x0.2 = 0.8 PMF) and 2 charges (2x0.8=1.6))

We follow the model of Bernard Korzeniewski [9] which was also taken over by Daniel A. Beard [8] of a linear dependence of the rate upon the difference of potential near equilibrium:

VCIII = VM_CIII * ΔECIII.

ΔECIII (for two electrons) decomposes into a $\Delta ECIII_{Chem}$ =2(EC – EQ[SR1]) which accounts for the chemical part of the reaction and –2.4 * PMF (Volts) corresponding to the protons and charges transported on either side of the inner mitochondrial membrane

ΔECIII = 2(EC – EQ) – 2.4.PMF = 2 ([EC_0 + RT/F *ln(Cox/Cred)] – [EQ_0 + RT/2F*ln(Q/QH2)]) – 2.4.PMF

With EC_0 (standard potential of Cred/Cox) = + 0.25 V and EQ_0 (standard potential of Q/QH2) = +0.085 V and with RT/F. ln(10) = 0.06 V at 30°C, we obtain:

ΔECIII = 2[0.25 + 0.06.$\log_{10}$(Cox/Cred) – (0.085+ 0.03. $\log_{10}$(Q/QH2)] – 2.4.PMF

Linearly written the equation reads:
VM_CIII*(0.50+0.12*$\log_{10}$(Cox/Cred))-(0.17+0.06*$\log_{10}$(Q/QH2))-2.4*PMF)

RCIV or Cytochrome c oxidase.

We take an equation close to that of Korzeniewski ((6)): $\frac{VM_{CIV}.Cred}{\frac{KO}{O_2}+1}$ modulated by a sigmoid function: $\frac{Kslip}{PMF^{Pslip}+Kslip}$ to take into account the H^+ slip at the level of complex IV as a function of the PMF. This function exchange a transduction of 3.6 H^+ to 1.6 H^+ around 0.2 V.

SUCCINATE THIOKINASE or SUCCINYL-COA SYNTHETASE (SUCTHIOK):

SUCCoAm + ADPm + Pim = SUCCm + ATPm + CoAm

We consider this equation as reversible with KQ_STK = 1.3 integrated in the mass action law equation:

ODC1 or ODC2 (Oxo-dicarboxylate carrier)

T2: AKGc + MALm = AKGm + MALc . (ODC)

Mass action reversible

T6: PYRm -> PYRc + 0.2 PMF

Mass action irreversible

T22: AKGc + SUCCm = AKGm + SUCCc . (ODC)

Mass action reversible

T23: AKGc + CITm = AKGm + CITc (ODC)

Mass action reversible

As an indication, Odc1 exchanges the following internal metabolites against AKG ext (with the corresponding rate in mmol.min/mg prot): AKG (112), Malate (56), Succinate (19) . [11]

DIC (Dicarboxylate carrier)

T31: MALm + Pic = MALc + Pim .

Mass action reversible

T33: SUCCc + Pim = SUCCm + Pic .

Mass action reversible

S3. EFMs with entry of AKG, ADP, Pi and O and output of ATP.

EFMs

4: (12) [bl 1] (10 ANT) -ASYNT (-13 IDH3) (13 SUCTHIOK) (10 T5) (-10 T12) (-26 T24) (-10 T41) (10 T42) (13 AKGDH) (13 T22) (13 T23) irreversible

17: (13) [bl 1] ANT RC3 SUCTHIOK T5 -T12 -T24 -T41 T42 AKGDH (5 L) NDI RC4 T22 irreversible. ATP/O = 1

20: (15) [bl 1] ANT FUMARASE (2 RC3) SUCTHIOK T5 -T12 -T24 -T41 T42 AKGDH (11 L) NDI RC2 (2 RC4) T2 irreversible ATP/O = 0.5

23: (16) [bl 1] ANT FUMARASE -IDH3 RC3 SUCTHIOK T5 -T12 (-2 T24) -T41 T42 AKGDH (5 L) RC2 RC4 T2 T23 irreversible ATP/O = 1

28: (13) [bl 1] (28 ANT) (5 ASYNT) (13 RC3) (13 SUCTHIOK) (28 T5) (-28 T12) (-13 T24) (-28 T41) (28 T42) (13 AKGDH) (13 NDI) (13 RC4) (13 T22) irreversible. Echange AKGc/SUCCm avec chemin AKGm – SUCCoAm – SUCCm qui sort ATP/O = 2.15

29: (15) [bl 1] (46 ANT) (11 ASYNT) (13 FUMARASE) (26 RC3) (13 SUCTHIOK) (46 T5) (-46 T12) (-13 T24) (-46 T41) (46 T42) (13 AKGDH) (13 NDI) (13 RC2) (26 RC4) (13 T2) irreversible ATP/O = 1.77

30: (16) [bl 1] (28 ANT) (5 ASYNT) (13 FUMARASE) (-13 IDH3) (13 RC3) (13 SUCTHIOK) (28 T5) (-28 T12) (-26 T24) (-28 T41) (28 T42) (13 AKGDH) (13 RC2) (13 RC4) (13 T2) (13 T23) irreversible Echange AKGc/MALm et AKGC/CITm. Pas production de NADH. Seul RC2 ATP/O = 2.15

42: (14) [bl 1] (6 ANT) (-5 IDH3) RC3 (6 SUCTHIOK) (6 T5) (-6 T12) (-11 T24) (-6 T41) (6 T42) (6 AKGDH) NDI RC4 (6 T22) (5 T23) irreversible

43: (16) [bl 1] (6 ANT) FUMARASE (-6 IDH3) RC3 (6 SUCTHIOK) (6 T5) (-6 T12) (-12 T24) (-6 T41) (6 T42) (6 AKGDH) RC2 RC4 T2 (5 T22) (6 T23) irreversible

OVERALL REACTIONS

4: - 10 ADP + 26 AKG + 10 Pi = 10 ATP + 13 CITc + 13 SUCCc (no O)
17: 1 ADP + AKG + O + Pi = ATP + CO2 + H2O + SUCCc
20: 0.5 ADP + AKG + 2 O + Pi = ATP + CO2 + 2 H2O + MALc
23: 1 ADP + 2 AKG + O + Pi = ATP + CITc + H2O + MALc
28: 2.15 28 ADP + 13 AKG + 13 O + 28 Pi = 28 ATP + 13 CO2 + 13 H2O + 13 SUCCc
29: 1.77 46 ADP + 13 AKG + 26 O + 46 Pi = 46 ATP + 13 CO2 + 26 H2O + 13 MALc
30: 2.15 28 ADP + 26 AKG + 13 O + 28 Pi = 28 ATP + 13 CITc + 13 H2O + 13 MALc
42: 6 6 ADP + 11 AKG + O + 6 Pi = 6 ATP + 5 CITc + CO2 + H2O + 6 SUCCc
43: 6 6 ADP + 12 AKG + O + 6 Pi = 6 ATP + 6 CITc + H2O + MALc + 5 SUCCc

Supplementary Materials S4 : Parameters of the kinetic model :

Model	**MITOY_AKG_12_**	**reduit_v3_TM_ ASYNT.cps**	
Z	0.06	(LEAK).Z mmol/l	0.06
DGP	0.37472	(T2).k1 l/(mmol*s)	1
nA	3.3	(ND1).k1 l/(mmol*s)	1
DG_SN	0.555204	(RCII).VM_SDH mmol/(l*s)	4.8
Gamma	1.79E+09	(RCII).KSDH_SUCC mmol/l	0.463514
fmu	0.8	(RCII).KiSDH_OAA mmol/l	0.108692
DPSI	0.225436	(RCII).KSDH_Q mmol/l	0.00495077
DPH	0.939317	(RCII).KQ_SDH 1	70
Ac	5.00E-13	(RCII).KSDH_FUM mmol/l	0.337697
Am	0.0483731	(RCII).KSDH_QH2 mmol/l	0.002
fPSI	0.8	(T22).k1 l/(mmol*s)	0.4
Nm	0.229722	(T31).k1 l/(mmol*s)	0
fp	0.2	(T33).k1 l/(mmol*s)	0
Phi_p	7.15676	(CS).VM_CS mmol/(l*s)	11.5

ATP/O	1.84327	(CS).KCS_OAA mmol/l	0.005
(AKGDH).VM_AKGDH $l^2/(mmol^2*s)$	340	(CS).KCS_ACOA mmol/l	0.01
(AKGDH).KAKGdh_NADH mmol/l	0.03	(CS).KQ_CS 1	2.00E+06
(AKGDH).KAKGdh_SucCoA mmol/l	0.01	(CS).KiCS_ATP mmol/l	0.3
(SUCTHIOK).VM_STK $l^2/(mmol^2*s)$	6.97225	(CS).KCS_CIT mmol/l	3
(SUCTHIOK).KQ_STK 1	1.3	(CS).KCS_COA mmol/l	0.04
(FUMARASE).VM_FUM mmol/(l*s)	12.5478	(IDH3).VM_IDH3 mmol/(l*s)	5.8
(FUMARASE).KFUMASE_FUM mmol/l	0.004	(IDH3).KI3_CIT mmol/l	3.2
(FUMARASE).KQ_FUMASE 1	4	(IDH3).KI3_NAD mmol/l	0.2
(FUMARASE).KFUMASE_MAL mmol/l	0.009	(IDH3).KQ_IDH3 1	7
(ASYNT).VM_ASYNT mmol/(l*s)	0	(IDH3).KI3_AKG mmol/l	9
(ASYNT).PMFa mmol/l	0.15	(IDH3).KI3_NADH mmol/l	0.7
(ASYNT).Phi_p mmol/l	7.15676	(MDH2).k1 l/(mmol*s)	20
(ASYNT).Z ?	0.06	(MDH2).k2 l/(mmol*s)	100000
(ASYNT).nA ?	3.3	(ME2).k1 l/(mmol*s)	0
(ANT).VM_ANT l/(mmol*s)	0.2	(ME2).k2 $l^2/(mmol^2*s)$	0
(ANT).fmu l/mmol	0.8	(PDH).VMPDH mmol/(l*s)	7
(Pit).VM_Pit mmol/(l*s)	200	(PDH).KPDHPYR mmol/l	0.025
(Pit).Z mmol/l	0.06	(PDH).KPDHNAD mmol/l	0.05
(ATPASE).VM_ATPASE mmol/(l*s)	0.05	(PDH).KiNADH mmol/l	0.036
(ATPASE).KATPASE_ATP mmol/l	3.57734	(PDH).KPDHCoAm mmol/l	0.013
(RCIII).VM_CIII mmol/(l*s)	1	(PDH).KiACoA mmol/l	0.035
(RCIV).VM_CIV 1/s	1	(T6).k1 l^4/(mmol^4*s)	1
(RCIV).KO mmol/l	0.001	(T24).k1 1/s	100
(LEAK).VM_Leak mmol/(l*s)	1.00E-06	(T24).k2 1/s	100
		(T23).k1 l/(mmol*s)	0.6

References

1. Bohnensack, R. Control of Energy Transformation of Mitochondria. Analysis by a Quantitative Model. *Biochim Biophys Acta* **1981**, *634*, 203–218, doi:10.1016/0005-2728(81)90139-0.
2. Yang, L.; Garcia Canaveras, J.C.; Chen, Z.; Wang, L.; Liang, L.; Jang, C.; Mayr, J.A.; Zhang, Z.; Ghergurovich, J.M.; Zhan, L.; et al. Serine Catabolism Feeds NADH When Respiration Is Impaired. *Cell Metab.* **2020**, *31*, 809-821.e6, doi:10.1016/j.cmet.2020.02.017.
3. Hamada, M.; Koike, K.; Nakaula, Y.; Hiraoka, T.; Koike, M. A Kinetic Study of the Alpha-Keto Acid Dehydrogenase Complexes from Pig Heart Mitochondria. *J Biochem* **1975**, *77*, 1047–1056, doi:10.1093/oxfordjournals.jbchem.a130805.
4. Smith, C.M.; Bryla, J.; Williamson, J.R. Regulation of Mitochondrial Alpha-Ketoglutarate Metabolism by Product Inhibition at Alpha-Ketoglutarate Dehydrogenase. *J Biol Chem* **1974**, *249*, 1497–1505.
5. Henri Victor Theorie Generale de l'action de Quelques Diastases. *C R Hebd Seances Acad Sci 135, 916–919* 1902.
6. Cornish-Bowden A; Hofmeyr J. Enzymes in context: Kinetic characterization of enzymes for systems biology. The Biochemist April 2005: 11-14. Available online: https://www.qwant.com/ (accessed on 27 June 2021).
7. König, M.; Bulik, S.; Holzhütter, H.-G. Quantifying the Contribution of the Liver to Glucose Homeostasis: A Detailed Kinetic Model of Human Hepatic Glucose Metabolism. *PLoS Comput Biol* **2012**, *8*, e1002577, doi:10.1371/journal.pcbi.1002577.
8. Grivennikova, V.G.; Gavrikova, E.V.; Timoshin, A.A.; Vinogradov, A.D. Fumarate Reductase Activity of Bovine Heart Succinate-Ubiquinone Reductase. New Assay System and Overall Properties of the Reaction. *Biochim Biophys Acta* **1993**, *1140*, 282–292, doi:10.1016/0005-2728(93)90067-p.
9. Korzeniewski, B.; Zoladz, J.A. A Model of Oxidative Phosphorylation in Mammalian Skeletal Muscle. *Biophysical Chemistry* **2001**, *92*, 17–34, doi:10.1016/S0301-4622(01)00184-3.
10. Beard, D.A. A Biophysical Model of the Mitochondrial Respiratory System and Oxidative Phosphorylation. *PLoS Comput Biol* **2005**, *1*, e36, doi:10.1371/journal.pcbi.0010036.
11. Palmieri, L.; Agrimi, G.; Runswick, M.J.; Fearnley, I.M.; Palmieri, F.; Walker, J.E. Identification in Saccharomyces Cerevisiae of Two Isoforms of a Novel Mitochondrial Transporter for 2-Oxoadipate and 2-Oxoglutarate. *J Biol Chem* **2001**, *276*, 1916–1922, doi:10.1074/jbc.M004332200.